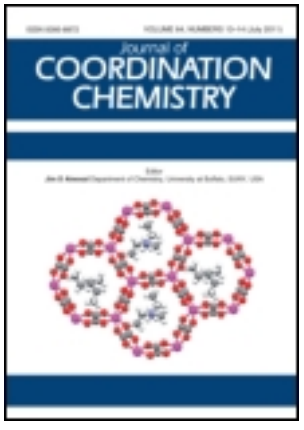

Journal of Coordination Chemistry
Publication details, including instructions for authors and subscription information:
http://www.tandfonline.com/loi/gcoo20

Anion mediated formation of different Schiff bases from the same precursors and their nickel(II) complexes with different nuclearity

Averi Guha [a], Arpita Banerjee [a], Raju Mondol [b], Ennio Zangrando [c] & Debasis Das [a]

[a] Department of Chemistry, University of Calcutta, 92, A. P. C. Road, Kolkata - 700009, India

[b] Department of Chemistry, IACS, Kolkata - 700032, India

[c] Dipartimento di Scienze Chimiche e Farmaceutiche, University of Trieste, Via L. Giorgieri 1, Trieste 34127, Italy

Published online: 04 Nov 2011.

To cite this article: Averi Guha, Arpita Banerjee, Raju Mondol, Ennio Zangrando & Debasis Das (2011) Anion mediated formation of different Schiff bases from the same precursors and their nickel(II) complexes with different nuclearity, Journal of Coordination Chemistry, 64:22, 3872-3886, DOI: 10.1080/00958972.2011.632413

To link to this article: http://dx.doi.org/10.1080/00958972.2011.632413

Journal of Coordination Chemistry
Vol. 64, No. 22, 20 November 2011, 3872–3886

Anion mediated formation of different Schiff bases from the same precursors and their nickel(II) complexes with different nuclearity

AVERI GUHA†, ARPITA BANERJEE†, RAJU MONDOL‡, ENNIO ZANGRANDO§ and DEBASIS DAS*†

†Department of Chemistry, University of Calcutta, 92, A. P. C. Road, Kolkata – 700009, India
‡Department of Chemistry, IACS, Kolkata – 700032, India
§Dipartimento di Scienze Chimiche e Farmaceutiche, University of Trieste, Via L. Giorgieri 1, Trieste 34127, Italy

(*Received 26 July 2011; in final form 29 September 2011*)

Two nickel(II) complexes, $[Ni_2L^1_2(H_2O)_4](NO_3)_2$ (**1**) and $[Ni_5L^2_2(OAc)_6(OH)_2]\cdot 5.5H_2O$ (**2**), have been synthesized and structurally characterized by X-ray crystallographic study, where L^1 and L^2 represent 2-formyl-4-methyl-6-(1-(2-aminomethyl)piperidine)-iminomethylphenolate and 4-methyl-2,6-bis(1-(2-aminomethyl)piperidine)-iminomethylphenolate, respectively. One-pot reactions between 2,6-diformyl-4-methylphenol with 1-(2-aminoethyl)piperidine, in the presence of nickel(II) nitrate and nickel(II) acetate, afforded *in situ* [1 + 1] and [1 + 2] condensation leading to Schiff-bases HL^1 and HL^2, and to **1** and **2** of different nuclearity. Both processes were conducted under the same reaction conditions in anhydrous EtOH. Preferential attainment of bi- or pentanuclear compounds is mediated by the anion of the Ni(II) salt. Complex **1** is formed by two unsymmetrical tridentate L^1 chelating in a head-tail fashion to make a centrosymmetric phenoxido-bridged Ni(II) dimer. Two waters complete octahedral coordination. Conversely in **2**, two $[Ni_2(OAc)L^2]^+$ units, having a *syn-syn* bidentate bridging acetate, embrace a third Ni through bridging acetate and μ_3-hydroxide, giving rise to an adduct of C_2 symmetry where the compartmental ligand planes form a dihedral angle of *ca.* 82°. The catecholase activity of these complexes were explored and both complexes effectively catalyze the conversion of 3,5-di-*tert*-butylcatechol (3,5-DTBC) to 3,5-di-*tert*-butylbenzoquinone (3,5-DTBQ).

Keywords: Polynuclear Ni(II) complex; Catecholase activity; Crystal structure; Schiff-base ligand

1. Introduction

Transition metal complexes with two or more metals in close proximity are of interest as models of active centers of metal-containing proteins, molecular magnets, and potential components of homogeneous catalytic systems [1–9]. Multinuclear transition and rare earth metal complexes also have attracted interest for their multi-electron redox reactivity for substrates and ferromagnetic or antiferromagnetic properties [10–13].

*Corresponding author. Email: dasdebasis2001@yahoo.com

ISSN 0095-8972 print/ISSN 1029-0389 online © 2011 Taylor & Francis
http://dx.doi.org/10.1080/00958972.2011.632413

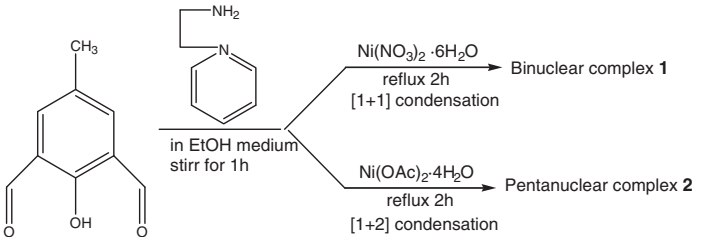

Scheme 1. Schematic view of the formation of the two complexes.

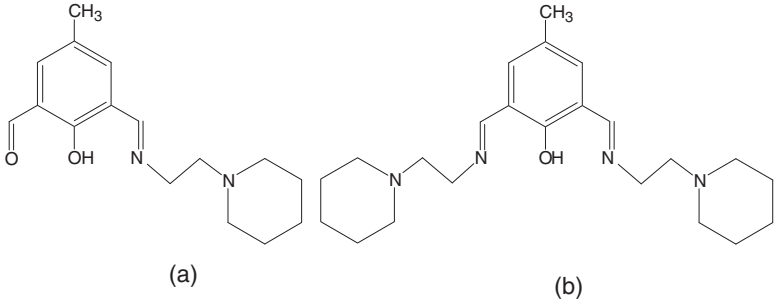

Scheme 2. Chemical structure of HL^1 (a) and HL^2 (b).

Recent years have witnessed an explosion of interest in design, synthesis and potential application of polynuclear molecules and molecule-based coordination polymers of different dimensionality in material science [14–23].

Despite interest in such complexes, synthetic methods have yet to reach the level of efficiency attained with mononuclear complexes. Polynuclear complexes require appropriate choice of ligand systems and Schiff bases may serve this purpose. Generally, Schiff base formation depends on the nature of the amine, the carbonyl moiety and of their relative stoichiometry. Although polynuclear Ni clusters with acetate [24, 25], perchlorate [26] or azido anions [27] have been described, no report on the catalytic influence of the metal salt was described. Here we report *in situ* formation of $1+1$ and $1+2$ condensed Schiff bases (schemes 1 and 2) starting from 2,6-diformyl-4-methylphenol and 1-(2-aminoethyl)piperidine mediated by acetate or nitrate Ni(II) salts and on the corresponding di- and penta-nuclear metal complexes. The syntheses (scheme 1) were conducted with a one-pot template condensation reaction in anhydrous EtOH. Surprisingly by using nickel(II) nitrate, a $[1+1]$ Schiff-base condensation takes place with formation of a binuclear complex, whereas nickel(II) acetate led to a $[1+2]$ condensation between the precursors giving a pentanuclear complex. We also tried other anions, SO_4^{2-}, Cl^-, and PO_4^{3-}, etc., but no solid products can be isolated. The catecholase activity of these complexes were also studied using 3,5-DTBC as substrate.

2. Experimental

2.1. *Starting materials*

Solvents were dried according to standard procedure and distilled prior to use. 2,6-Diformyl-4-methylphenol was prepared according to the literature method [28].

1-(2-Aminoethyl)piperidine (Aldrich), nickel(II) nitrate hexahydrate (Merck) and nickel(II) acetate tetrahydrate (Loba Chemie) were purchased from commercial sources and used as received. All other chemicals were of AR grade.

2.2. *Physical measurements*

Elemental analyses (carbon, hydrogen, and nitrogen) were performed using a Perkin Elmer 240 C elemental analyzer. Infrared spectra (4000–400 cm^{-1}) were recorded at 300 K using a Shimadzu FTIR-8400 S with KBr. Electronic spectra (1500–300 nm) were obtained at 25°C using a Hitachi U-3501 spectrophotometer in acetonitrile. EPR analysis was performed at 77 K using methanol glass and spectra in the X band were recorded with a JEOL JESFA200 spectrometer.

2.3. *Syntheses of the complexes*

2.3.1. Complex 1: $[Ni_2L^1_2(H_2O)_4](NO_3)_2$ (1). The complex was prepared by adding dropwise an ethanolic solution of $Ni(NO_3)_2 \cdot 6H_2O$ (0.727 g, 2.5 mmol) over the Schiff base formed *in situ* between 2,6-diformyl-4-methylphenol and 2-(2-aminoethyl)piperidine (1 : 2) in anhydrous ethanol with stirring over 2 h and the mixture was maintained at reflux for 1 h. The mixture was filtered at its boiling point and the filtrate evaporated at atmospheric pressure until solid started to appear. After cooling, the green precipitate was collected by filtration to give the binuclear nickel(II) complex. The binuclear nickel(II) complex was dissolved in ethanol/acetone (30 mL, 1 : 1) and the solution was slowly evaporated to give green single crystals of the binuclear nickel(II) complex (figure 1a). Yield: 69%. Anal. Calcd for $C_{32}H_{50}N_6O_{14}Ni_2$ (**1**): C, 44.68; H, 5.86; N, 9.77. Found: C, 44.53; H, 5.66; N, 9.62%.

2.3.2. Complex 2: $[Ni_5L^2_2(OAc)_6(OH)_2]$ (2). Was synthesized by adopting a similar procedure as for **1** where $Ni(OAc)_2 \cdot 4H_2O$ (0.6221 g, 2.5 mmol) was used instead of $Ni(NO_3)_2 \cdot 6H_2O$ to give the pentanuclear nickel(II) complex (figure 2a). Yield: 71%. Anal. Calcd for $C_{58}H_{90}N_8O_{16}Ni_5$ (**2**): C, 48.08; H, 6.26; N, 7.73. Found: C, 48.01; H, 6.03; N, 7.55%.

2.4. *X-ray crystal structure determinations*

Diffraction data for **1** (at 120(2) K) and **2** (room temperature) were collected on a Bruker Smart Apex diffractometer equipped with a CCD detector and Mo-Kα radiation ($\lambda = 0.71073$ Å). Cell refinement, indexing and scaling of the data sets were carried out using Bruker Smart Apex and Bruker Saint packages [29]. The structures were solved by direct methods and subsequent Fourier analyses [30] and refined by full-matrix least-squares based on F^2 with all observed reflections [30]. The contribution of hydrogens at calculated positions was introduced in the final cycles of refinement, except those of water located on the ΔF map and refined restraining the O–H distances at 0.85 Å. The coordinating piperidine (N4) in **2** is disordered over two conformations

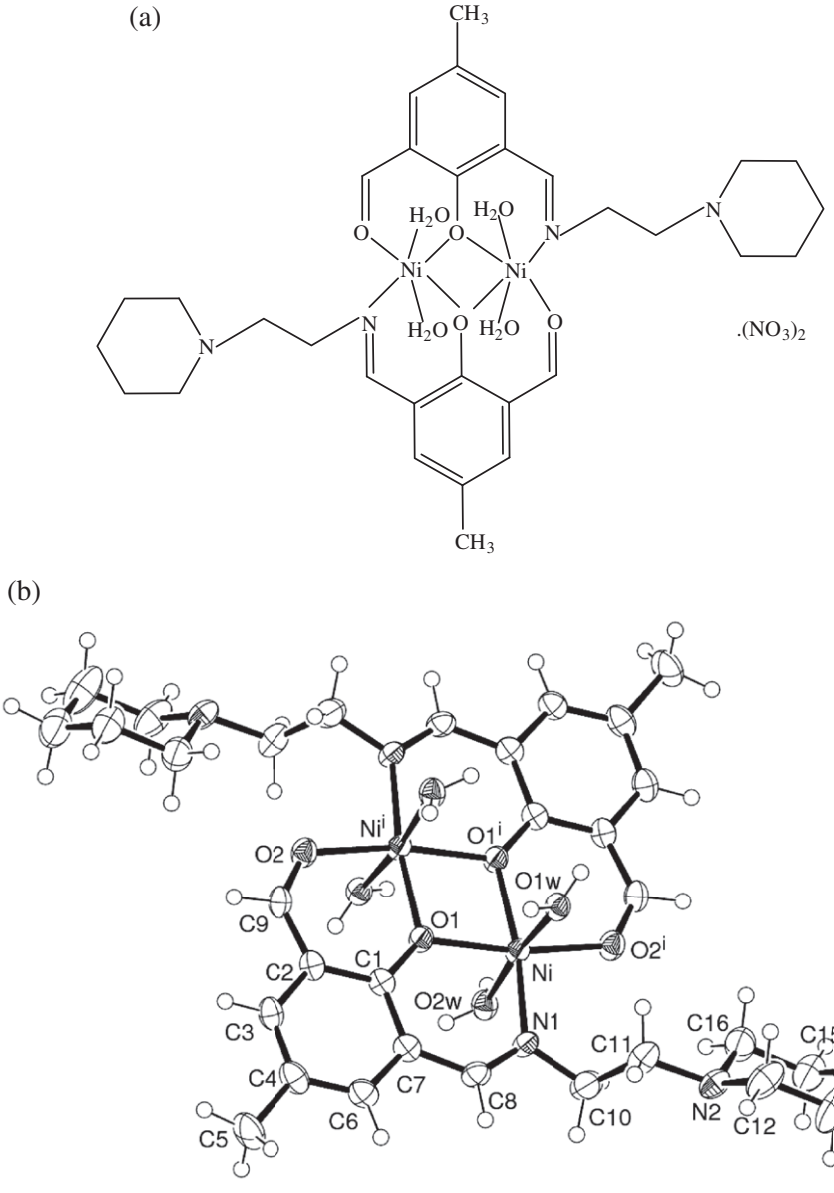

Figure 1. (a) Chemical structure of **1**; (b) ORTEP drawing (50% probability ellipsoid) of the molecular cation of **1** with atom labels of the independent part.

(occupancy of 0.50 each). Some residuals in the ΔF map were successfully refined as an acetic acid molecule (0.50 occupancy) and as four water oxygens (two at full occupancy, the other at 0.50 and 0.25 occupancy, no hydrogens located). Crystallographic data and details of refinements are reported in table 1. All the calculations were performed using the WinGX System, Ver 1.80.05 [31].

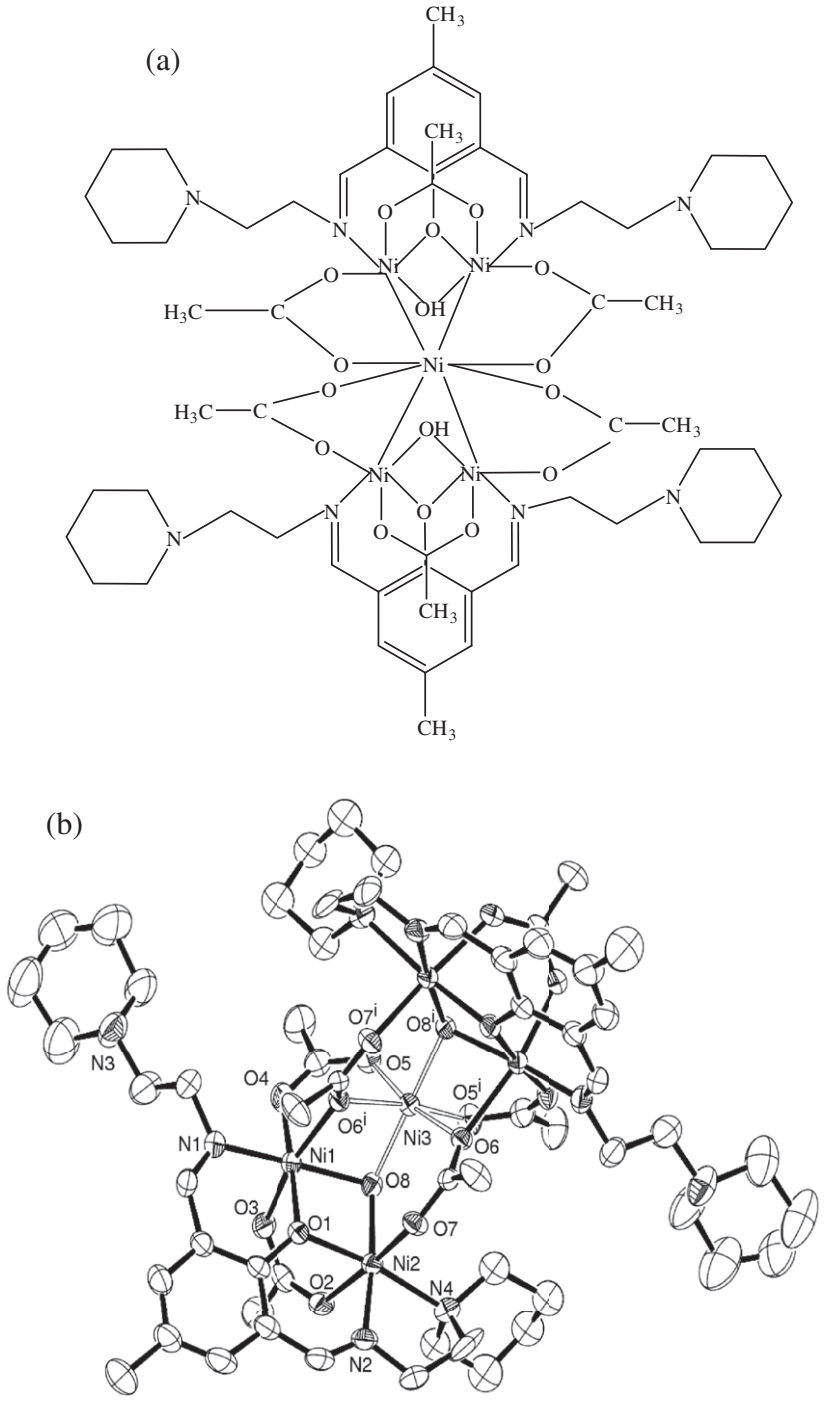

Figure 2. (a) Chemical structure of **2**; (b) ORTEP drawing (35% probability ellipsoid) of the pentanuclear **2** of C_2 symmetry (only the coordinated atoms labeled for the sake of clarity and for disordered piperidine ring N4, only one orientation is shown).

Table 1. Crystallographic data and details of structure refinements for **1** and **2**.

	1	**2**
Empirical formula	$C_{32}H_{50}N_8Ni_2O_{20}$	$C_{60}H_{105}N_8Ni_5O_{23.50}$
Formula weight	984.22	1608.07
Crystal system	Monoclinic	Monoclinic
Space group	$P2_1/c$	$C2/c$
Unit cell dimensions (Å, °)		
a	14.5801(4)	18.1844(19)
b	10.1560(3)	15.5834(19)
c	14.0143(4)	27.789(3)
β	92.4720(10)	103.798(2)
Volume (Å^3), Z	2073.24(10), 2	7647.4(15), 4
Calculated density (g cm^{-3})	1.577	1.397
Absorption coefficient (mm^{-1})	0.998	1.283
$F(000)$	1028	3396
θ_{max} (°)	25.99	25.15
Reflections collected	25,697	21,677
Independent reflection	4078 [R(int) = 0.0416]	6646 [R(int) = 0.0780]
Observed $I > 2\sigma(I)$	3338	4696
Parameters	293	473
Goodness-of-fit on F^2	1.047	1.043
Final R indices ($I > 2\sigma(I)$)[a]	$R_1 = 0.0463$, $wR_2 = 0.1255$	$R_1 = 0.0607$, $wR_2 = 0.1843$
Largest difference peak and hole (e Å^{-3})	1.164 and −0.503	1.003 and −0.561

[a] $R_1 = \Sigma||F_o|-|F_c||/\Sigma|F_o|$, $wR_2 = [\Sigma w(F_o^2 - F_c^2)^2/\Sigma w(F_o^2)^2]^{1/2}$.

3. Results and discussion

3.1. *Syntheses and characterization*

Complex **1** is prepared by applying template synthesis treating nickel(II) nitrate hexahydrate with the Schiff base formed *in situ* between 2,6-diformyl-4-methylphenol and 1-(2-aminoethyl)piperidine in anhydrous ethanol. Complex **2** is prepared following same procedure as for **1** by using nickel(II) acetate tetrahydrate instead. The ratio of diformyl, amine and nickel(II) salt was maintained as 1 : 2 : 2.5. We performed the reaction changing the above ratio to 1 : 1 : 2.5 and 1 : 1 : 5. In each case we obtained the same complexes. Complexes **1** and **2** show bands in IR spectra at 1639 cm^{-1} due to C=N stretch and skeletal vibrations at 1543–1591 cm^{-1}. Complex **1** has a band at 1384 cm^{-1} due to NO_3^- [32]. Complex **2** shows a band centered at 1037 cm^{-1} due to acetate. Electronic spectra of both complexes show three peaks corresponding to octahedral Ni(II) as given in "Supplementary material". Effective magnetic moments at 300 K and the expected spin only values are collected in table 2. The spin only values were calculated by using the equation $\mu_{Ni} = 2[S_{Ni}(S_{Ni}+1)]^{1/2}$ for mononuclear complexes thus $\mu_{Ni-Ni} = [2\mu_{Ni}^2]^{1/2}$ for dinuclear **1** and $\mu_{Ni-Ni} = [5\mu_{Ni}^2]^{1/2}$ for pentanuclear **2**. The effective magnetic moment of **1** agrees with that predicted for a high spin d^8 nickel(II) and that of pentanuclear **2** is also in agreement with corresponding spin only value suggesting no strong magnetic interaction between metal ions. Being a non-Kramer's ion, nickel(II) ion may exhibit EPR signal at low temperatures. We have performed EPR experiment with our nickel(II) complexes at 77 K in methanol glass and both complexes are EPR active. Complex **1** exhibits a very complicated EPR spectrum

Table 2. Effective magnetic moments of **1** and **2**.

Complex	Effective magnetic moment (μ_{eff}/μ_B)	Expected spin only value ($\mu_{spinonly}/\mu_B$)
1	3.94	4.00
2	5.96	6.32

Table 3. Selected bond lengths (Å) and angles (°) for **1**.

Ni–O(1)	2.004(2)	Ni–N(1)	2.015(2)
Ni–O(1′)	2.023(2)	Ni–O(1w)	2.086(2)
Ni–O(2′)	2.016(2)	Ni–O(2w)	2.092(2)
O(1)–Ni–N(1)	91.34(10)	O(2′)–Ni–O(1w)	88.51(9)
O(1)–Ni–O(2′)	169.42(9)	O(1′)–Ni–O(1w)	92.77(9)
N(1)–Ni–O(2′)	99.21(10)	O(1)–Ni–O(2w)	92.73(9)
O(1)–Ni–O(1′)	80.65(9)	N(1)–Ni–O(2w)	85.96(10)
N(1)–Ni–O(1′)	171.86(10)	O(2′)–Ni–O(2w)	88.82(9)
O(2′)–Ni–O(1′)	88.82(9)	O(1′)–Ni–O(2w)	92.95(9)
O(1)–Ni–O(1w)	90.95(9)	O(1w)–Ni–O(2w)	173.63(9)
N(1)–Ni–O(1w)	88.77(10)	Ni–O(1)–Ni′	99.35(9)

Primed atoms $-x+2, -y, -z+1$.

with six split signals (Supplementary material) having $g_3 = 2.15911$, $g_2 = 2.0126275$ and $g_1 = 1.85085$. Complex **2** shows a less complicated spectrum (Supplementary material) with $g_3 = 2.45554$, $g_2 = 2.30073$ and $g_1 = 1.98743$. The g value is isotropic and close to 2×2. In general, if the zero-field splitting (D) is negligible, one would expect and observe a single EPR line. However, in most of the systems, D is non-zero and hence more than one line has been observed.

3.2. *Description of crystal structures*

Crystal structure analysis of **1** reveals a dinuclear complex cation and nitrate anions. The complex, located on a crystallographic inversion center, is formed by two unsymmetrical tridentate ligands that chelate nickel in a head-tail arrangement, creating a phenoxido-bridged Ni(II) dimer. An ORTEP view of the complex cation of **1** with atom labeling is shown in figure 1(b), and a selection of bond lengths and angles is given in table 3. The metals, separated by 3.0702(7) Å, exhibit octahedral coordination, with two phenoxido-bridged oxygens, an imine nitrogen and a carbonyl oxygen, completing the coordination sphere with two waters at axial positions. The complex has coplanar phenols with piperidine rings (showing a chair conformation) far from the metal center. The Ni–N and Ni–O bond distances in the equatorial plane are comparable in length ranging from 2.004(2) to 2.023(2) Å, whereas the waters have slightly longer distances of 2.086(2) and 2.092(2) Å. The crystal packing shows nitrates H-bonded to water (O···O distance of *ca* 2.78 Å) forming 2D layers parallel to crystallographic planes (100) (figure 3).

In **2** the pentanuclear species can be described as formed by two $[Ni_2(OAc)L^2]$ units connected to a third Ni through bridging acetate and μ_3 hydroxides (figure 2b); selected bond distances and angles for **2** are given in table 4. All three independent Ni

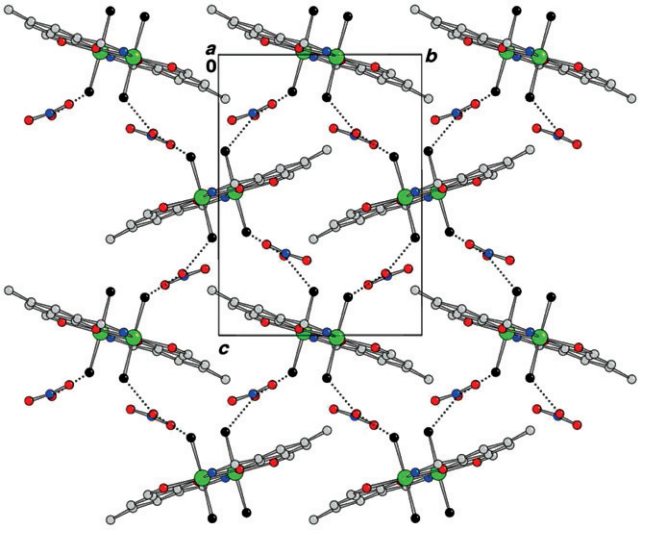

Figure 3. Crystal packing of **1**: 2-D network formed by H-bonds occurring between water and nitrate (piperidine rings not shown for the sake of clarity).

Table 4. Selected bond lengths (Å) and angles (°) for **2**.

Ni(1)–O(1)	2.029(3)	Ni(2)–O(8)	2.013(4)
Ni(1)–O(3)	2.067(4)	Ni(2)–N(2)	2.000(5)
Ni(1)–O(4)	2.050(4)	Ni(2)–N(4)	2.179(5)
Ni(1)–O(6′)	2.137(3)	Ni(3)–O(8)	2.006(3)
Ni(1)–O(8)	2.034(3)	Ni(3)–O(5)	2.049(4)
Ni(1)–N(1)	2.038(5)	Ni(3)–O(6)	2.095(3)
Ni(2)–O(1)	2.035(3)	Ni(1)–Ni(2)	2.9581(10)
Ni(2)–O(2)	2.120(4)	Ni(1)–Ni(3)	3.0773(7)
Ni(2)–O(7)	2.060(3)	Ni(2)–Ni(3)	3.6227(8)
O(1)–Ni(1)–O(3)	89.69(15)	O(7)–Ni(2)–O(2)	174.85(16)
O(1)–Ni(1)–O(4)	176.27(15)	O(8)–Ni(2)–O(2)	88.66(15)
O(1)–Ni(1)–O(6′)	93.75(13)	O(2)–Ni(2)–N(2)	89.48(17)
O(1)–Ni(1)–O(8)	85.09(14)	O(2)–Ni(2)–N(4)	91.75(17)
O(1)–Ni(1)–N(1)	88.61(17)	O(8)–Ni(2)–O(7)	92.17(13)
O(3)–Ni(1)–O(4)	86.61(17)	O(7)–Ni(2)–N(2)	89.20(16)
O(3)–Ni(1)–O(6′)	166.38(14)	O(7)–Ni(2)–N(4)	93.01(17)
O(3)–Ni(1)–O(8)	89.24(14)	O(8)–Ni(2)–N(2)	174.23(18)
O(3)–Ni(1)–N(1)	94.98(17)	O(8)–Ni(2)–N(4)	102.86(16)
O(4)–Ni(1)–O(6′)	89.96(15)	N(2)–Ni(2)–N(4)	82.7(2)
O(4)–Ni(1)–O(8)	95.29(15)	O(5)–Ni(3)–O(5′)	84.6(2)
O(4)–Ni(1)–N(1)	91.27(18)	O(6)–Ni(3)–O(6′)	92.83(19)
O(6′)–Ni(1)–O(8)	77.94(13)	O(8′)–Ni(3)–O(8)	173.98(19)
O(6′)–Ni(1)–N(1)	98.27(16)	O(5)–Ni(3)–O(6)	169.85(14)
O(8)–Ni(1)–N(1)	172.40(17)	O(5)–Ni(3)–O(6′)	92.01(15)
O(1)–Ni(2)–O(2)	85.85(14)	O(5′)–Ni(3)–O(8)	91.08(16)
O(1)–Ni(2)–O(7)	89.15(14)	O(5)–Ni(3)–O(8)	93.38(15)
O(8)–Ni(2)–O(1)	85.47(14)	O(6′)–Ni(3)–O(8)	79.54(13)
O(1)–Ni(2)–N(2)	88.95(17)	O(6)–Ni(3)–O(8)	96.26(13)
O(1)–Ni(2)–N(4)	171.29(16)	Ni(1)–O(1)–Ni(2)	93.42(14)

Primed atoms $-x+1, y, -z+1/2$.

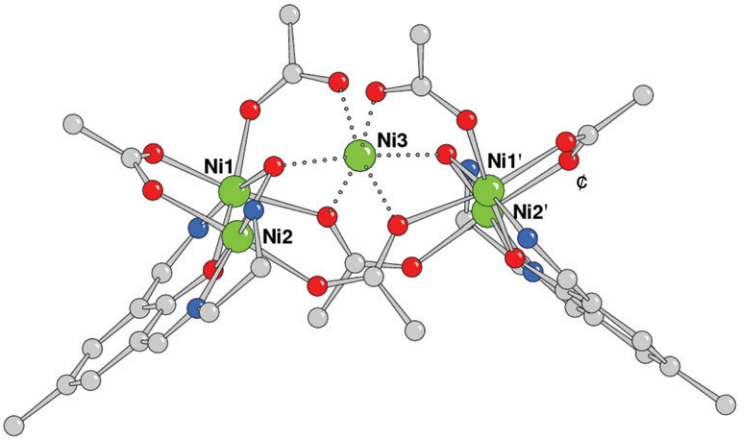

Figure 4. Side view of **2** (piperidine rings not shown for clarity).

ions have distorted octahedral geometry with different coordination. Ni(1) has a $\{O_5N\}$ coordination sphere provided by a μ_3-OH, bridging phenolate, three acetate oxygens and an imino nitrogen. Ni(2) is $\{O_4N_2\}$ provided by a μ_3-OH, bridging phenolate, two acetate oxygens, and the chelating amino- and imino-nitrogens. The central Ni(3) is six-coordinate ($\{O_6\}$ donor set) through two μ_3-hydroxides and four oxygens from bridging acetates. The central Ni resides on a crystallographic two fold axis with the compartmental ligands forming a dihedral angle of 82.4(1)°. Two acetate linkers connect Ni(3) with $[Ni_2(OAc)L^2]$ fragments as *syn-syn* bidentate bridging and two as $\eta^2\mu_3$ triply bridging ligands (operative inside the convex angle formed by phenolato rings (figure 4).

Within the compartmental ligand the distance between Ni(1) and Ni(2) is 2.958(1) Å, while the intermetallic Ni(2)–Ni(3) and Ni(1)–Ni(3) separations are 3.6227(8) and 3.0773(7) Å, respectively. The longer intermetallic distance is induced by steric factors, since it occurs between Ni(3) and Ni(2), the latter being chelated by the imino-amino fragment. This feature has been reported in other pentanuclear Ni clusters. Here the metals chelated by the Schiff base are a bit closer than in **1** (3.0702(7) Å), with a corresponding Ni(1)–O(1)–Ni(2) phenoxide bridge angle of 93.42(14)° (in **1** 99.35(9)°). The O–H groups, μ_3-bridging the Ni_3 isosceles triangle and displaced by 0.71 Å from the metal plane, represent a key functional species beside acetate to give this pentanuclear cluster.

The Ni–O distances range from 2.013(4) to 2.137(3) Å, while the Ni–N bond lengths fall between 2.000(5)–2.179(5) Å, being the longest for a piperidine nitrogen donor. **2** resembles complexes reported by Fenton *et al.* [24], with asymmetric compartmental ligands as well as ligands bearing a carbonyl instead of the preformed imine [25]. In all these cases the Ni_5 core has a comparable architecture, although with a narrower angle between the mean planes through phenolate (54–64° to be compared with the value of 82° measured in **2**). It is difficult to access if this feature is due to the different compartmental ligands or rather to packing requirements.

The crystallographic analysis shows the presence of 5.5 disordered lattice waters and one acetic acid per complex unit. Most of these fill channels down the (101) direction formed by packing of the complexes, as shown figure 5.

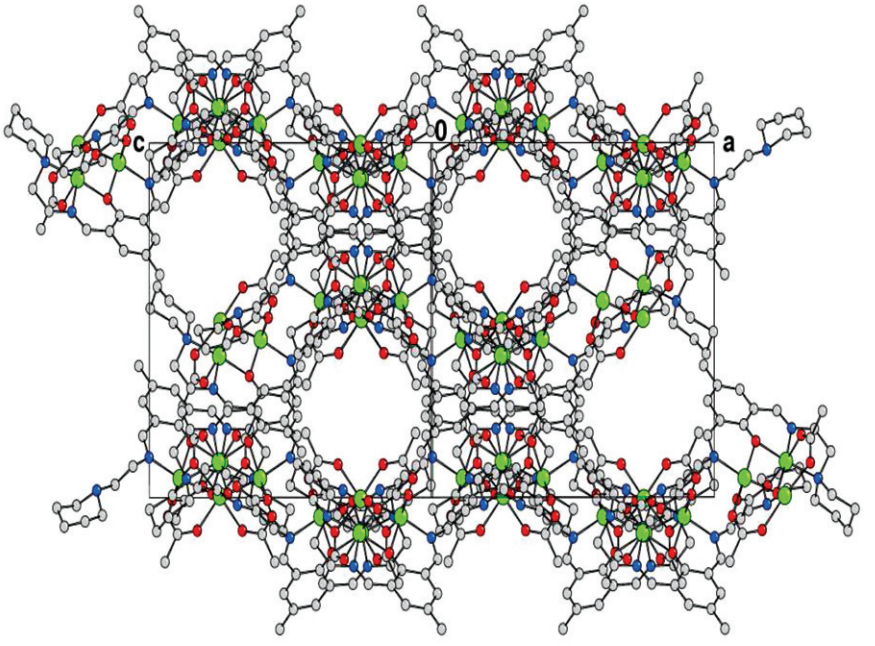

Figure 5. Crystal packing of **2** showing channel parallel to (101) direction.

3.3. *Catechol oxidase activity*

The ubiquitous plant enzyme catechol oxidase is a Type-3 active site copper protein where copper is surrounded by three nitrogens from histidine residues [33, 34]. This protein reversibly binds dioxygen at ambient conditions and utilizes it to perform the oxidation of phenolic substrates to o-quinones, which later were tested as models of catechol oxidase enzyme and can catalyze the reaction for conversion of 3,5-di-*tert*-butylcatechol (3,5-DTBC) to 3,5-di-*tert*-butylbenziquinone (3,5-DTBQ) that was studied in MeOH with UV-Vis spectroscopy.

3,5-DTBC has no absorption in the region of 390 nm, but on reaction between the catalyst and the substrate in a 1:100 ratio in air saturated methanol, a band appeared at 390 nm and 397 nm for **1** and **2**, respectively. Thus both complexes catalyze formation of *o*-quinone from catechol. The absorbances at 390 nm and 397 nm increased with time showing an augmented formation of quinone from catechol. For **2** the increase at 397 nm followed for 60 min is more enhanced than for **1**, indicating a more rapid conversion of 3,5-DTBC to 3,5-DTBQ. On the other hand the solid state structures of the complexes (described above) suggest that **1** should favor conversion of 3,5-DTBC to 3,5-DTBQ over **2**, but we obtain the opposite result and, to access the apparent contradiction, performed ESI-MS experiments to evaluate the structures of the complexes in methanol. Complex **1** exhibits a base peak at 724.20 amu, which corroborates well with mono positive species of composition $[Ni_2(L1)_2(NO_3)] + (m/z$, Calcd 724.07 amu). In contrast, the analysis of ESI-MS spectrum for **2** reveals a base peak at 617.16 amu corresponding to a dinuclear species of probable composition $[Ni_2L_2(OAc)_2(0.5H_2O)] + (m/z$, Calcd 616.57 amu) from fragmentation of the

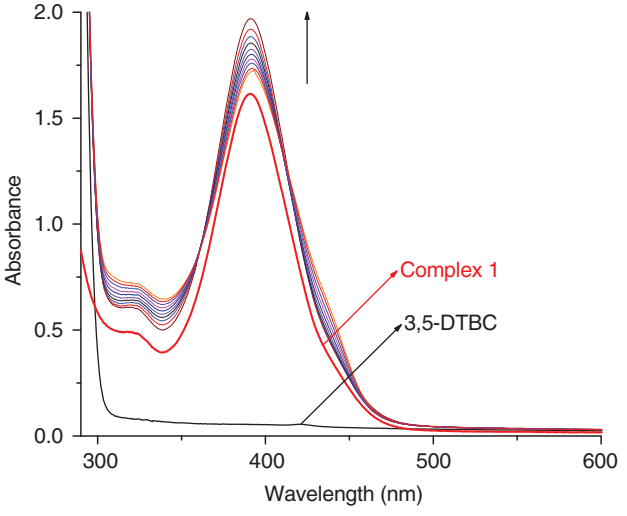

Figure 6. UV-Vis spectra (300–800 nm): (i) **1** (1×10^{-4} mmol) in methanol; (ii) 3,5-DTBC (1×10^{-2} mmol) in methanol; (iii) changes in UV-Vis spectra of **1** upon the addition of 100-fold 3,5-DTBC observed at regular time intervals.

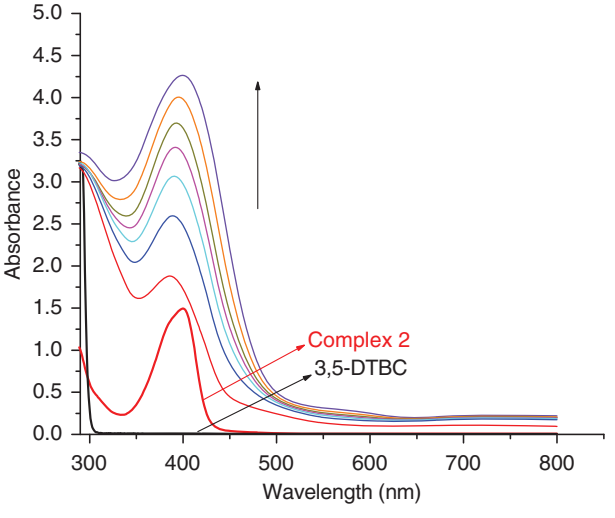

Figure 7. UV-Vis spectra (300–800 nm): (i) **2** (1×10^{-4} mmol) in methanol; (ii) 3,5-DTBC (1×10^{-2} mmol) in methanol; (iii) changes in UV-Vis spectra of **2** upon the addition of 100-fold 3,5-DTBC observed at regular time intervals.

pentanuclear complex and a peak at 1331 amu related to $[Ni_4(L_2)_2(OAc)_5(H_2O)]+$ (m/z, Calcd 1332.12 amu) in a very small percentage in methanol (ESI-MS spectra reported in "Supplementary material"). Therefore, mass spectral analyses suggest that in methanol pentanuclear **2** fragments into two nickel(II) species, whereas the dinuclear **1** remains intact. Thus, under equal molar concentrations of **1** and **2**, the latter generates catalytically active species and consequently shows better activity in converting

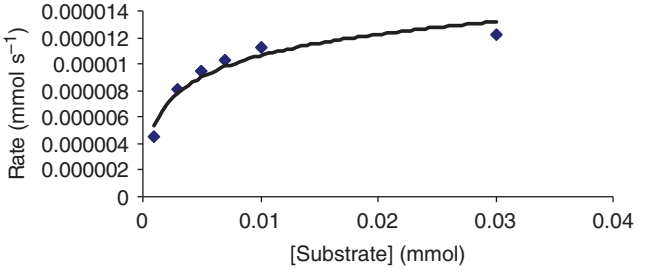

Figure 8. Enzyme kinetics data for **1** with 3,5-DTBC in methanol.

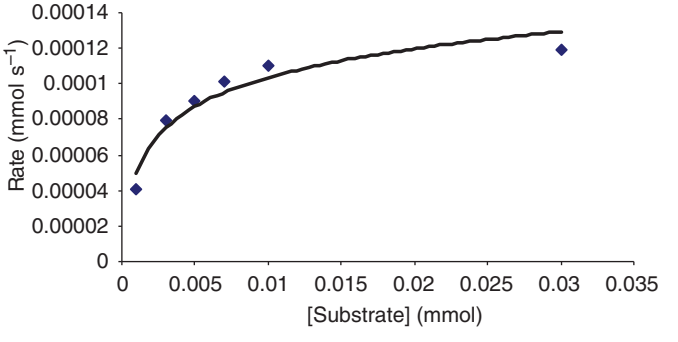

Figure 9. Enzyme kinetics data for **2** with 3,5-DTBC in methanol.

3,5-DTBC to 3,5-DTBQ with rate of conversion 10 times faster using **2** as the catalyst as revealed from kinetic experiments. Figures 6 and 7 represent the time dependent spectral change of **1** and **2**, respectively, upon addition of 3,5-DTBC.

The kinetics for oxidation of 3,5-DTBC was determined by the initial rate method at 25°C. The concentration of 3,5-DTBC was always kept at least 10 times larger than that of the Ni^{II} complex and the increase of 3,5-DTBQ concentration was determined at 390 nm for **1** and 397 nm for **2**. Solutions of 3,5-DTBC with concentrations ranging from 0.001 to 0.05 mol dm^{-3} were prepared from a concentrated stock solution in MeOH and MeCN separately. 2 mL of the substrate solution was poured in a 1 cm quartz cell thermostated at 25°C. Then 0.04 mL of 0.005 mol dm^{-3} Ni^{II} complex solution was quickly added so that the ultimate concentrations of Ni^{II} complex becomes 1×10^{-4} mol dm^{-3}.

The dependences of the initial rates on the concentration of substrate monitored spectrophotometrically are given in figures 8 and 9. The values of K_m and V_{max} were calculated for **1** and **2** from graphs of $1/V$ *versus* $1/[S]$ (given in figure 10) known as the Lineweaver–Burk plot by using the equation $1/V = \{K_m/V_{max}\}\{1/[S]\} + 1/V_{max}$.

The complexes exhibit a considerable catecholase-type activity by catalyzing oxidation of DTBC to DTBQ. The initial rate method shows a first-order dependence on complex concentration exhibiting saturation kinetics at higher DTBC concentrations. For this reason, treatment based on the Michaelis–Menten model was

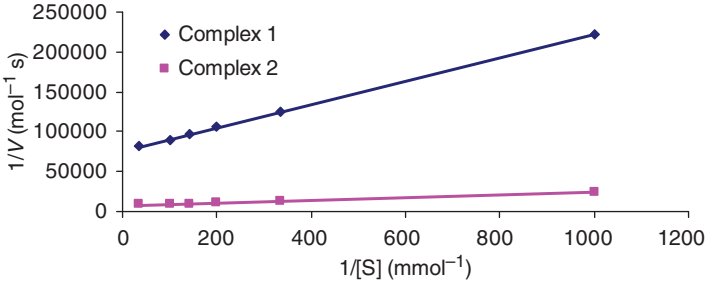

Figure 10. The Lineweaver–Burk plots (double reciprocal plot) for **1** and **2** in methanol.

Table 5. Kinetic parameters for catecholase activity of **1** and **2** in MeOH.

Complex	Wavelength (nm)	V_{max} (mmol s^{-1})	K_m (mmol)	k_{cat} (h^{-1})
1	390	1.32×10^{-5}	1.93×10^{-3}	4.74×10^{1}
2	397	1.32×10^{-4}	2.21×10^{-3}	4.77×10^{2}

deemed appropriate. Figure 10 represents the Lineweaver–Burk plots (double reciprocal plot) for the complexes in methanol.

The Lineweaver–Burk plots (figure 10) evaluate complex parameters, such as maximum velocity (V_{max}), Michaelis binding constant (K_m), rate constant for the dissociation of substrate (i.e., turnover number, k_{cat}) in MeOH. The data are listed in table 5.

4. Conclusions

This work demonstrates that [1 + 1] or [1 + 2] condensed Schiff-base formations are mediated by the anion of the nickel salt. In particular, the coordination ability of acetate drives the synthesis towards pentanuclear Ni_5 complex with compartmental ligands having symmetric imine groups, while in presence of nitrates binuclear complex is obtained from Schiff-base ligands with a carbonyl instead of the preformed imine. Both complexes exhibit catecholase-like activity in oxidizing 3,5-DTBC to 3,5-DTBQ under aerobic conditions with the pentanuclear species showing better efficiency.

Supplementary material

CCDC reference numbers 812393 and 812394 contain the supplementary crystallographic data for **1** and **2**, respectively. These data can be obtained free of charge from the Cambridge Crystallographic Data Centre via www.ccdc.cam.ac.uk/data_request/cif, or E-mail: deposit@cdc.cam.ac.uk.

Acknowledgments

The authors wish to thank the University Grants Commission, New Delhi [UGC Major Research Project, F. No. 34-308\2008 (SR) Dated: 31.12.2008 (DD)] for financial support. Averi Guha is thankful to Shailabala Biswas Research Foundation, University of Calcutta, for financial support.

References

[1] (a) R.H. Holm, E.I. Solomon. *Chem. Rev.*, **96**, 7 (1996); (b) R.H. Holm, E.I. Solomon. *Chem. Rev.*, **104**, 2 (2004).
[2] (a) S.J. Lippard, J.M. Berg, *Principles of Bioinorganic Chemistry*, University Science Books, Mill Valley, CA (1994); (b) K.D. Karlin, Z. Tyeklar, *Bioinorganic Chemistry of Copper*, Chapman & Hall, New York (1993).
[3] A. Messerschmidt, R. Huber, T. Poulos, K. Wieghardt. *Handbook of Metalloproteins*, John Wiley & Sons, Chichester, UK (2001).
[4] (a) D. Gatteschi, O. Kahn, J.S. Miller, F. Palacio, *Magnetic Molecular Materials*, Kluwer Academic Publishers, Dordrecht, The Netherlands (1991); (b) C.J. O'Connor, *Research Frontiers in Magnetochemistry*, World Scientific, Singapore (1993).
[5] O. Kahn. *Molecular Magnetism*, VCH, Weinheim, Germany (1993).
[6] (a) D. Gatteschi, R. Sessoli. *Angew. Chem., Int. Ed.*, **42**, 268 (2003); (b) G. Christou, D. Gatteschi, D.N. Hendrickson, R. Sessoli. *MRS Bull.*, **25**, 66 (2000).
[7] (a) J.L.C. Rowsell, O.M. Yaghi. *Angew. Chem. Int. Ed.*, **44**, 4670 (2005); (b) L. Jiang, H.J. Choi, X.L. Feng, T.B. Lu, J.R. Long. *Inorg. Chem.*, **46**, 2181 (2007).
[8] D.Y. Wu, O. Sato, C.Y. Duan. *Inorg. Chem. Commun.*, **12**, 325 (2009).
[9] (a) M. Dey, C. Rao, P.K. Saarenketo, K. Rissanen. *Inorg. Chem. Commun.*, **5**, 380 (2002); (b) F. Luo, J.M. Zheng, M. Kurmoo. *Inorg. Chem.*, **46**, 8448 (2007).
[10] E.I. Solomon, T.C. Brunold, M.I. Davis, J.N. Kemsley, K. Lee, N. Lehnert, F. Neese, A.J. Skulan, Y.S. Yang, J. Zhou. *Chem. Rev.*, **100**, 235 (2000).
[11] N.A. Law, M.T. Caudle, V.L. Pecoraro. *Adv. Inorg. Chem.*, **46**, 305 (1998).
[12] E. Kimura, T. Koike, S. Aoki. *Yuki Gosei Kagaku Kyokaishi*, **55**, 1052 (1997).
[13] X.M. Chen, Y.Y. Yang. *Chin. J. Chem.*, **18**, 664 (2000).
[14] J.H.J. Satcher, M.M. Olmstead, M.W. Droege, S.R. Parkin, B.C. Noll, L. May, A.L. Balch. *Inorg. Chem.*, **37**, 6751 (1998).
[15] P.E. Kruger, B. Moubaraki, G.D. Fallon, K.S. Murray. *J. Chem. Soc., Dalton Trans.*, **713**, 2000.
[16] C.J. Matthews, K. Avery, Z. Xu, L.K. Thompson, L. Zhao, D.O. Miller, K. Biradha, K. Poirier, M.J. Zaworotko, C. Wilson, A.E. Goeta, J.A.K. Howard. *Inorg. Chem.*, **38**, 5266 (1999).
[17] H. Yamashita, M. Koikawa, T. Tokii. *Mol. Cryst. Liq. Cryst. Sci., Sect. A*, **342**, 63 (2000).
[18] C. He, C.Y. Duan, C.J. Fang, Y.J. Liu, Q.J. Meng. *J. Chem. Soc., Dalton Trans.*, 1207 (2000).
[19] F. Estevan, A. Garcia-Bernabe, P. Lahuerta, M. Sanau, M.A. Ubeda, A.M.C. Ramirez. *Inorg. Chem.*, **39**, 5964 (2000).
[20] A.J. Edwards, B.F. Hoskins, R. Robson, J.C. Wilson, J. Moubaraki, K.S. Murray. *J. Chem. Soc., Dalton Trans.*, 1837 (1994).
[21] (a) A. Banerjee, R. Singh, E. Colacio, K.K. Rajak. *Eur. J. Inorg. Chem.*, 277 (2009); (b) C.J. Matthews, K. Avery, Z.Q. Xu, L.K. Thompson, L. Zhao, D.O. Miller, M.J. Zaworotko, K. Biradha, K. Poirier, C. Wilson, A.E. Goeta, J.A.K. Howard. *Inorg. Chem.*, **38**, 5266 (1999).
[22] (a) K. Yoneda, K. Adachi, K. Nishio, M. Yamasaki, A. Fuyuhiro, M. Katada, S. Kaizaki, S. Kawata. *Angew. Chem. Int. Ed.*, **45**, 5459 (2006); (b) X. Feng, L.Y. Wang, J.S. Zhao, J.G. Wang, B. Liu, X.G. Shi. *Inorg. Chim. Acta*, **632**, 5127 (2009).
[23] H.H. Monfared, J. Sanchiz, Z. Kalantari, C. Janiak. *Inorg. Chim. Acta*, **362**, 3791 (2009).
[24] H. Adams, S. Clunas, D.E. Fenton, D.N. Towers. *J. Chem. Soc., Dalton Trans.*, 3933 (2002).
[25] H. Adams, D.E. Fenton, P.E. McHugh. *Inorg. Chem. Commun.*, **7**, 880 (2004).
[26] H. Adams, S. Clunas, D.E. Fenton. *Chem. Commun.*, 418 (2002).
[27] D. Mandal, V. Bertolasi, J. Ribas-Ariño, G. Aromí, D. Ray. *Inorg. Chem.*, **47**, 3465 (2008).
[28] R.R. Gagne, C.L. Spiro, T.J. Smith, C.A. Hamann, W.R. Thies, A.K. Shiemeke. *J. Am. Chem. Soc.*, **103**, 4073 (1981).
[29] Bruker. *SMART, SAINT. Software Reference Manual Bruker AXS Inc.*, Madison, Wisconsin, USA (2000).

[30] G.M. Sheldrick. *Acta Cryst A*, **64**, 112 (2008).
[31] L.J. Farrugia. *J. Appl. Crystallogr.*, **32**, 837 (1999).
[32] K. Nakamoto. *Infrared and Raman Spectra of Inorganic and Coordination Compounds*, 3rd Edn, Wiley, New York (1978).
[33] E.I. Solomon, U.M. Sundaram, T.E. Machonkin. *Chem. Rev.*, **96**, 2563 (1996).
[34] E.I. Solomon, M.J. Baldwin, M.D. Lowery. *Chem. Rev.*, **92**, 521 (1992).